Research Article

# Short Channel Field-Effect Transistors from Highly Enriched Semiconducting Carbon Nanotubes

Justin Wu[1], Liming Xie[1], Guosong Hong[1], Hong En Lim[2], Boanerges Thendie[2], Yasumitsu Miyata[2], Hisanori Shinohara[2], and Hongjie Dai[1] (✉)

[1] Department of Chemistry, Stanford University, Stanford, CA 94305, USA
[2] Department of Chemistry and Institute for Advanced Research, Nagoya University, Nagoya 464-8602, Japan

## ABSTRACT

Semiconducting single-walled carbon nanotubes (s-SWNTs) with a purity of ~98% have been obtained by gel filtration of arc-discharge grown SWNTs with diameters in the range 1.2–1.6 nm. Multi-laser Raman spectroscopy confirmed the presence of less than 2% of metallic SWNTs (m-SWNTs) in the s-SWNT enriched sample. Measurement of ~50 individual tubes in Pd-contacted devices with channel length 200 nm showed on/off ratios of >$10^4$, conductances of 1.38–5.8 μS, and mobilities in the range 40–150 cm$^2$/(V·s). Short channel multi-tube devices with ~100 tubes showed lower on/off ratios due to residual m-SWNTs, although the on-current was greatly increased relative to the devices made from individual tubes.

## KEYWORDS

One of the long standing hurdles encountered in the practical use of carbon nanotubes for electronics is the surplus of chiral varieties produced by most methods of synthesis. The realization of high performance logic circuits requires s-SWNT field-effect transistors (FETs) exceeding current silicon counterparts. The presence of metallic nanotubes results in significantly lower on/off ratios and should be completely eliminated. Much experimental work has been performed recently to enrich s-SWNTs, and long channel thin-film transistors (TFTs) using these sorted tubes have been studied. Less work has been done on short channel devices due to the more stringent s-SWNT purity requirements.

In order to obtain single-walled carbon nanotube (SWNT) transistors with both high on-current and high on/off ratio [1–7], it is necessary to employ highly pure s-SWNTs with a suitable diameter range. Previous short channel FETs have used mostly semiconducting tubes with small diameters <1.1 nm [8–10]. Larger diameter SWNTs could afford higher mobility and higher on-state currents exceeding that of Si devices with similar width. There are currently a large number of approaches to enrich s-SWNTs, from manipulating growth conditions to preferentially grow semi-conducting tubes [11], to separation [12–15] and post-processing procedures that are intended to remove metallic nanotubes and render the materials insulating [16–20].

One of these approaches, solution phase separation,

---

Address correspondence to hdai1@stanford.edu

offers an effective way to purify carbon nanotubes to purities above 99% prior to deposition on a substrate. Gel filtration [14, 21–23], dielectrophoresis [24], density gradient ultracentrifugation [13, 25–26], and a variety of other methods [12, 27–29] have been employed for solution phase separation. While the performance of the thin films of SWNTs that can be formed from these techniques has been widely studied for long channel thin-film devices [30–32] much less work has been done to assess the purity of s-SWNTs and possible performance of short channel FETs composed of large numbers of s-SWNTs. This ideally requires 100% s-SWNT purity to achieve acceptable on/off ratios. Short channel FETs have been formed from solutions of semiconductors with extremely high purity [8, 10], and in one case, devices were formed of s-SWNTs with exclusively chirality (10, 5) and diameter 1.03 nm [9]. While these studies have shown the viability of these approaches for fabricating FET devices with respect to on/off ratios, the efficiency of separation and sorting has typically decreased in effectiveness as diameter has increased. Previous short channel FETs have used mostly semiconducting tubes with small diameters <1.1 nm, with consequently lower on-currents [33]. In this work, we investigated arc-discharge synthesized SWNTs with diameters 1.2–1.6 nm that had been repeatedly sorted via gel filtration to a purity of >98% [23].

The starting material was purified SWNTs produced by arc discharge (Meijo, Type-SO) dispersed in a solution of 1 wt.% sodium cholate. Sephacryl S-200 (GE Healthcare) was used as a gel filter for the separation. Prior to separation, an equal volume of 1 wt.% sodium dodecyl sulfate (SDS) was added to the solution. The solution was then passed through the gel; m-SWNTs were eluted by 1 wt.% SDS, and the s-SWNTs still trapped within the gel were then eluted with a 1 wt.% sodium cholate solution. For higher purity, the resulting solution was then passed multiple times through the gel in the same manner. A TFT with channel length 40 μm had mobility of 164 cm$^2$/(V·s) and on/off ratio of $10^6$. Normalized by the channel width of 200 μm, the device had a transconductance of 0.78 S/m [23].

Visible–near infrared (vis–NIR) absorption spectroscopy was first used to confirm that the $M_{11}$ peaks near 700 nm had been largely removed (Fig. 1(a)). One of our groups has previously estimated the purity of the semiconducting SWNTs obtained using this method to be near 99%, by comparison of their absorption properties with those reported by Engel et al. [26]. In this work, the SWNT solution was drawn into capillary tubes for solution phase Raman spectroscopy. Raman spectroscopy measurements were taken using a Horiba HR800 Raman system with 532, 633, and 785 nm excitation. Several peaks corresponding to nanotube radial breathing modes (RBM) were observed in the spectra [34, 35]. Under the 532 nm excitation, the RBM ($\omega_{RBM}$) was found at 170 cm$^{-1}$, corresponding to a s-SWNT with diameter ($d_t$) of 1.46 nm according to the equation $\omega_{RBM} = 248/d_t$ [36]. The 785 nm-excited Raman spectrum also contained a RBM metallic peak at 160 cm$^{-1}$. This peak shows that there are still metallic tubes present with diameters of ~1.55 nm. It should be noted that the intensities of the m-SWNT RBM peaks relative to those of the s-SWNT RBM peaks were very low compared to the values in the starting SWNT samples that had not been purified (Fig. 1(b)). Using the ratios of the intensity of the 785 nm-excited m-SWNT peak to the 532 nm-excited s-SWNT peak (8:1 in the as-made solution and 0.25:1 in the separated solution),
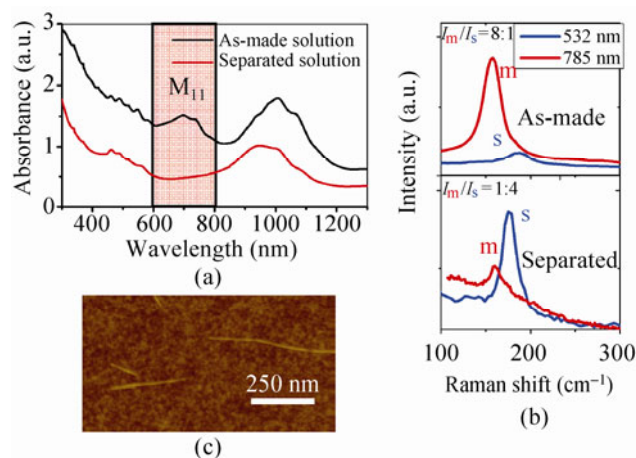


**Figure 1** (a) Absorption spectra of the as-made solution and the separated SWNT solution. (b) Solution-phase Raman spectra of the as-made solution (top panel) and separated SWNT solution (bottom panel) under 532 nm excitation and 785 nm excitation. Listed are the ratios of the s-SWNT RBM peak intensities under 532 nm excitation to the m-SWNT RBM peak intensities under 785 nm excitation. Raman measurement parameters were kept the same for the same excitation wavelength. (c) AFM image of the separated SWNT solution spun onto 300 nm SiO$_2$/Si

it was estimated that the percentage of m-SWNTs in the separated solution had decreased to ~1.1%, assuming the starting sample contained 33% m-SWNT. This purity estimate was consistent with that from the vis–NIR spectra.

In order to further assess the purity level as well as to measure some of the individual RBM peaks of tubes, the SWNT solution was deposited via drop-drying onto $SiO_2$/Si substrates (oxide thickness of 300 nm) which were then rinsed in water over 24 hours to help remove the residual surfactant. Samples were annealed at 900 ℃ in vacuum for 20 min to clean them. Raman mapping was then performed on areas densely populated with tubes (Figs. 2(a)–2(f)). Using 532 nm excitation, we observed a range of RBM peaks from 160 cm$^{-1}$ to 195 cm$^{-1}$, corresponding to s-SWNTs of 1.27 to 1.55 nm in diameter (Figs. 2(a) and 2(b)). Fewer peaks were found in the 633 nm measurements (Figs. 2(c) and 2(d)), including peaks at 153 cm$^{-1}$ and 171 cm$^{-1}$ corresponding to s-SWNTs, as well as peaks at 198 cm$^{-1}$ corresponding to m-SWNTs. Exciting the tubes at 785 nm reproduced the single peak at 160 cm$^{-1}$ found earlier (Figs. 2(e) and 2(f)). The rarity of these last two peaks over the mapping areas confirmed that the solution has been highly purified and enriched in s-SWNTs.

Atomic force microscopy (AFM) measurements of SWNT diameters confirmed that tubes with diameters of 1.2–1.6 nm were present in the sample (Fig. 1(c)). The mean of the distribution was found to be 1.4 nm; the majority of tubes were found to be between 1.3 nm and 1.5 nm. These results are consistent with the Raman spectra; the most common RBM peak found over the mapping areas corresponds to tubes with diameter ~1.4 nm.

Electrical devices were fabricated on $SiO_2$/Si (oxide thickness of 10 nm) substrates. In order to study both the performance of devices consisting of individual tubes as well as the performance of devices consisting of many tubes in parallel, the carbon nanotube solution was drop-dried as well as spin coated onto several substrates. As with the substrates studied by Raman spectroscopy, the samples were rinsed in water overnight and annealed in vacuum at 900 ℃ for 20 min. Individual tubes were identified and located by AFM imaging and contacted by 20 nm Pd electrodes defined by electron-beam lithography to form source and drain
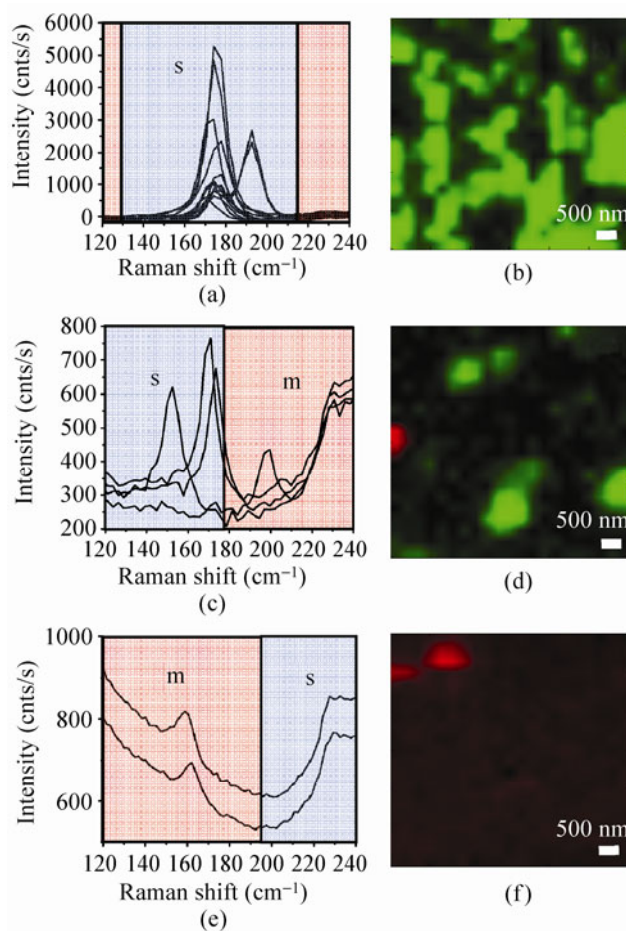


**Figure 2** Raman spectra of drop-dried SWNT samples on $SiO_2$/Si under (a) 532 nm, (c) 633 nm, and (e) 785 nm excitation. Areas of graph covered in blue mark Raman shifts corresponding to s-SWNT RBM peaks. Areas in red mark shifts corresponding to m-SWNT RBM peaks. The peak at ~225 cm$^{-1}$ is from the substrate. Raman mapping using (b) 532 nm, (d) 633 nm, and (f) 785 nm excitation. Areas containing s-SWNT RBM peaks are represented in green. Areas containing m-SWNT RBM peaks are shown in red

contacts spaced 200 nm apart. In order to improve the contact resistance, the devices were annealed in vacuum at 180 ℃ for 20 min [6]. Additional devices were made by random electrode deposition, and AFM imaging was used to select the devices with individual tubes. Multiple SWNT devices were lithographically defined without AFM imaging at channel lengths of 100 nm on the drop-dried samples.

The devices made from individual tubes had CNT diameters ranging from 1.23 nm to 1.50 nm as measured by AFM (Figs. 3(a) and 3(b)). Under ambient conditions, the conductance of the SWNT devices at 1 V bias voltage was found to range from 1.38 μS to

5.8 μS. This is comparable to previous measurements on CVD-grown tubes with diameters less than 1.5 nm, indicating that the separation and cleaning of the tubes had not resulted in additional damage to the tubes [6, 33]. Sub-threshold swings of the devices were found to range from 130 to 400 mV/dec. The on/off ratio was >10$^4$ for all of the single tube devices, indicating that of the individual tubes measured, none were metallic. The calculated effective mobilities of the tube devices ranged from 40–150 cm$^2$/(V·s) (the gate capacitance varied depending on the precise channel length; the average of the values calculated by three-dimensional (3D) electrostatic simulation for the nominal device was 7.24 aF) [37].

The calculated effective mobility was relatively low compared to the highest performance SWNT FETs based on $d$~1.7 nm SWNTs. This can be attributed to

the fact that Schottky barriers occurring at the contacts with nanotubes with diameter <1.5 nm reduced the amount of current that passed through the contacts into the tube [5, 6, 33]. It is also possible that defects still existed in these SWNTs within the 200 nm channel length.

Measurements of densely spaced multi-SWNT devices revealed different performances to those of the single tube devices (Figs. 3(c), 3(d), and 4(a)–4(c)). The number of tubes throughout the device was estimated by multiplying the film density near the devices (as measured by AFM) by the channel width. Although the on-current was substantially higher, as expected from a device consisting of multiple tubes, the on/off ratios for the devices were found to range from 3 to 10$^4$. The higher on/off ratios only occurred in devices with fewer than 15 tubes. On average, the
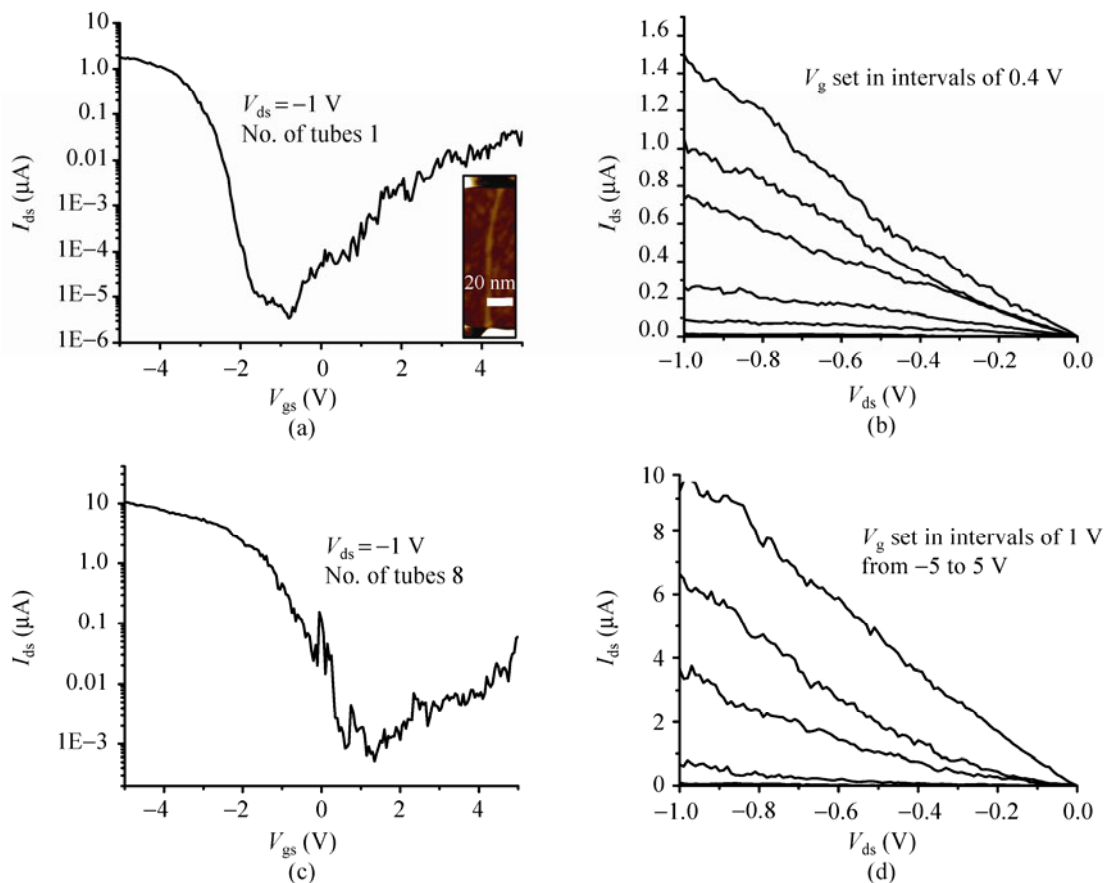


**Figure 3** (a) Source–drain current vs. backgate voltage ($I_{ds}$–$V_{gs}$) characteristics of a single SWNT device at 1 V source drain bias ($V_{ds}$) in vacuum. Inset: AFM image of the device. (b) $I_{ds}$–$V_{ds}$ characteristics of the same single SWNT device at $V_g$ in 0.4 V intervals from −5 to 5 V. (c) $I_{ds}$–$V_{gs}$ characteristics of a device connected by 8 SWNTs at $V_{ds}$ set to 1 V in ambient. (d) $I_{ds}$–$V_{ds}$ characteristics of the same device at $V_g$ at intervals of 1 V from −5 to 5 V

devices gained ~1.2 μA of on-current per additional tube. Several devices with ~10 μA on-current were able to maintain on/off ratios >$10^4$ (Fig. 3(c)). Devices with the number of tubes required to reach hundreds of μA had much lower on/off ratios (Figs. 4(a) and 4(b)). In order to investigate the cause of the low on/off
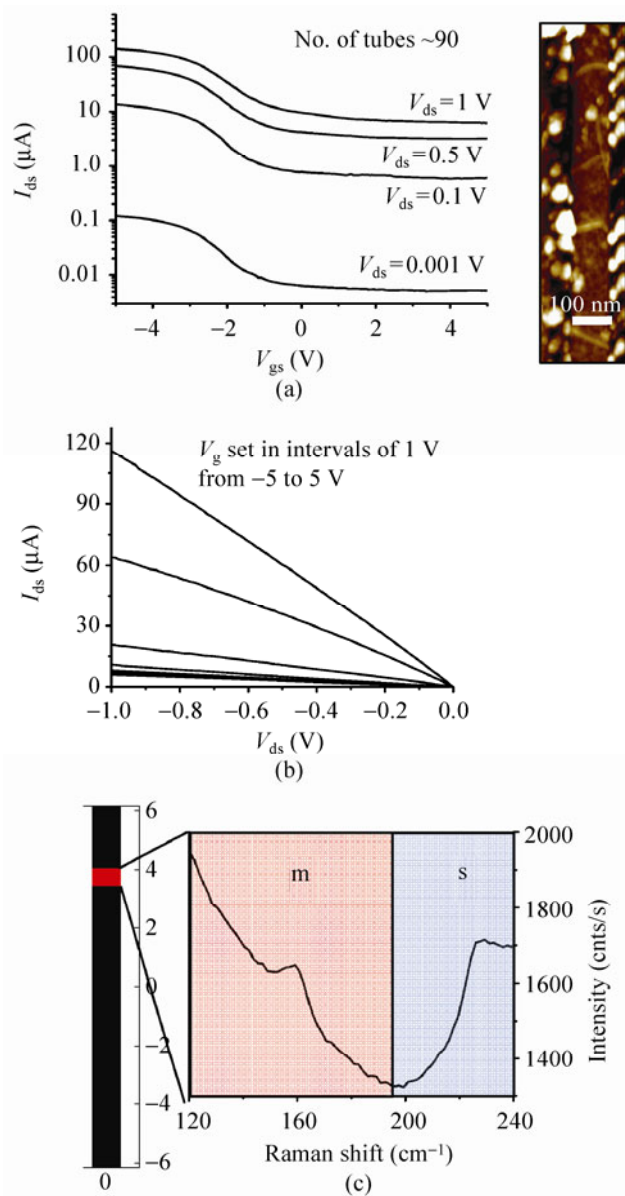
ratios for the large-number multiple tube devices, Raman spectroscopy was performed on the tubes within the channel area. Although the signal strength was considerably weakened due to the substantially thinner dielectric of 10 nm oxide, measurements on several devices revealed the presence of metallic tubes within the channel (Fig. 4(c)). In Fig. 4(c), a RBM peak found under the 785 nm excitation revealed the presence of a 1.55 nm metallic nanotube that causes the on/off ratio to drop significantly.

In comparison to previous work on short channel multiple CNT devices based on separated SWNTs ($d < 1.1$ nm) [8–10], the larger diameter of the individual SWNTs used here ($d \sim 1.4$ nm) resulted in smaller bandgaps ( >750 meV vs. >600 meV) [35], which led to lower Schottky barriers and higher mobility allowing for better performance on a per tube basis [7]. This decreases the number of tubes in the channel needed for a given on-current. Devices with ~10 tubes showed better on-currents and comparable on/off ratios to devices composed of fewer or similar numbers of tubes to those in earlier reports. This is indicative of s-SWNT tubes with similar purities, but with larger currents per tube. Compared to the (10, 5) SWNTs, for example, the average current per tube at $V_{ds} = -1$ V is ~5 times higher (~1.2 μA to ~0.25 μA) [9]. It should be noted that the device performance is still worse than that of large diameter ~1.7–2.0 nm SWNT FETs, which were capable of achieving on-currents of 20 μA with on/off ratios of $10^5$ for individual semiconducting SWNT devices [6]. While a s-SWNT purity of ~99% is sufficient to obtain currents of tens of μA without metallic tubes within the channel, larger currents cannot yet be reliably obtained without incurring low on/off ratios. It is therefore still necessary to increase the purity of s-SWNTs to 100%, in order to obtain high performance, short channel SWNT FETs for advanced electronics applications.

In summary, we have investigated the purity and electrical properties of highly enriched semiconducting SWNTs with an average diameter of ~1.4 nm. Investigation with Raman spectroscopy of the SWNTs both in solution and deposited on a substrate confirmed the low percentage of m-SWNTs. Measurements on individual tubes in fabricated Pd contacted devices with channel length 200 nm showed conductances from 1.38 μS to 5.8 μS as well as mobilities from



**Figure 4** (a) Source-drain current vs. backgate voltage ($I_{ds}$–$V_{gs}$) characteristics of a multiple SWNT device at 1 V source drain bias ($V_{ds}$) in ambient. Right: AFM image of part of the device. (b) $I_{ds}$–$V_{ds}$ characteristics of the same multiple SWNT device at $V_g$ spaced at 1 V from −5 to 5 V. (c) Left: Raman mapping of device channel under 785 nm excitation. m-SWNT RBM peak in red. Right: Raman spectra corresponding to the area in red. ~225 cm$^{-1}$ peak is from the substrate

40–150 cm²/(V·s), with high on/off ratios, comparable to those in previous work using tubes of this diameter. Short channel multiple tube devices showed that although the on-current using separated arc tubes could be increased to hundreds of μA, the on/off ratios were substantially lower, even for high percentages of semiconducting SWNTs. Raman mapping of the device channels confirmed that the reason for the lower ratios was the presence of residual metallic tubes within the device. The use of highly purified arc-discharge tubes is a step forward from previous work with tubes of diameter <1 nm, giving substantially higher current per tube in single and multiple tube devices. Ideally, the diameter range of enriched s-SWNT solutions needs to be pushed further towards 1.6–1.8 nm while further increasing purity. This will allow high yields of high performance SWNT FETs with high on/off ratios and currents of hundreds of μA to be reliably fabricated.

## References

[1]  Tans, S. J.; Verschueren, A. R. M.; Dekker, C. Room-temperature transistor based on a single carbon nanotube. *Nature* **1998**, *393*, 49–52.

[2]  Martel, R.; Schmidt, T.; Shea, H. R.; Hertel, T.; Avouris, P. Single- and multi-wall carbon nanotube field-effect transistors. *Appl. Phys. Lett.* **1998**, *73*, 2447–2449.

[3]  Zhou, C.; Kong, J.; Dai, H. Electrical measurements of individual semiconducting single-walled carbon nanotubes of various diameters. *Appl. Phys. Lett.* **2000**, *76*, 1597–1599.

[4]  Bachtold, A.; Hadley, P.; Nakanishi, T.; Dekker, C. Logic circuits with carbon nanotube transistors. *Science* **2001**, *294*, 1317–1320.

[5]  Appenzeller, J.; Knoch, J.; Derycke, V.; Martel, R.; Wind, S.; Avouris, P. Field-modulated carrier transport in carbon nanotube transistors. *Phys. Rev. Lett.* **2002**, *89*, 126801.

[6]  Javey, A.; Guo, J.; Wang, Q.; Lundstrom, M.; Dai, H. Ballistic carbon nanotube field-effect transistors. *Nature* **2003**, *424*, 654–657.

[7]  Dai, H.; Javey, A.; Pop, E.; Mann, D.; Kim, W.; Lu, Y. Electrical transport properties and field effect transistors of carbon nanotubes. *Nano*, **2006**, *1*, 1–13.

[8]  Zhang, L.; Zaric, S.; Tu, X.; Wang, X.; Zhao, W.; Dai, H. Assessment of chemically separated carbon nanotubes for nanoelectronics. *J. Am. Chem. Soc.* **2008**, *130*, 2686–2691.

[9]  Zhang, L.; Tu, X.; Welsher, K.; Wang, X.; Zheng, M.; Dai, H. Optical characterizations and electronic devices of nearly pure (10,5) single-walled carbon nanotubes. *J. Am. Chem. Soc.* **2009**, *131*, 2454–2455.

[10] Park, S.; Lee, H. W.; Wang, H.; Selvarasah, S.; Dokmeci, M. R.; Park, Y. J.; Cha, S. N.; Kim, J. M.; Bao, Z. Highly effective separation of semiconducting carbon nanotubes verified via short-channel devices fabricated using dip-pen nanolithography. *ACS Nano* **2012**, *6*, 2487–2496.

[11] Ding, L.; Tselev, A.; Wang, J.; Yuan, D.; Chu, H.; McNicholas, T. P.; Li, Y.; Liu, J. Selective growth of well-aligned semiconducting single-walled carbon nanotubes. *Nano Lett.* **2009**, *9*, 800–805.

[12] Zheng, M.; Jagota, A.; Semke, E. D.; Diner, B. A.; Mclean, R. S.; Lustig, S. R.; Richardson, R. E.; Tassi, N. G. DNA-assisted dispersion and separation of carbon nanotubes. *Nat. Mater.* **2003**, *2*, 338– 342.

[13] Arnold, M. S.; Stupp, S. I.; Hersam, M. C. Enrichment of single-walled carbon nanotubes by diameter in density gradients. *Nano Lett.* **2005**, *5*, 713–718.

[14] Takeshi, T.; Jin, H.; Miyata, Y.; Kataura, H. High-yield separation of metallic and semiconducting single-wall carbon nanotubes by agarose gel electrophoresis. *Appl. Phys. Express* **2008**, *1*, 114001.

[15] Hersam, M. C. Progress towards monodisperse single-walled carbon nanotubes. *Nat. Nanotechnol.* **2008**, *3*, 387–394.

[16] Yang, C. M.; An, K. H.; Park, J. S.; Park, K. A.; Lim, S. C.; Cho, S. H.; Lee, Y. S.; Park, W.; Park, C. Y.; Lee, Y. L. Preferential etching of metallic single-walled carbon nanotubes with small diameter by fluorine gas. *Phys. Rev. B* **2006**, *73*, 075419.

[17] Zhang, G.; Qi, P.; Wang, X.; Lu, Y.; Li, X.; Tu R.; Bansalruntip, S.; Mann, D.; Zhang, L.; Dai, H. Selective etching of metallic carbon nanotubes by gas-phase reaction. *Science* **2006**, *314*, 974–977.

[18] Kang, S. J.; Kocabas, C.; Ozel, T.; Shim, M.; Pimparkar, N.; Alam, M. A.; Rotkin, S. V.; Rogers, J. A. High-performance electronics using dense, perfectly aligned arrays of single-walled carbon nanotubes. *Nat. Nanotechnol.* **2007**, *2*, 230–236.

[19] Gomez, L. M.; Kumar, A.; Zhang, Y.; Ryu, K.; Badmaev, A.; Zhou, C. Scalable light-induced metal to semiconductor conversion of carbon nanotubes. *Nano Lett.* **2009**, *9*, 3592–3598.

[20] Kanungo, M.; Lu, H.; Malliaras, G. G.; Blanchet, G. B. Suppression of metallic conductivity of single-walled carbon nanotubes by cycloaddition reactions. *Science* **2009**, *323*, 234–237.

[21] Moshammer, K.; Hennrich, F.; Kappes, M. M. Selective suspension in aqueous sodium dodecyl sulfate according to electronic structure type allows simple separation of metallic from semiconducting single-walled carbon nanotubes. *Nano Res.* **2009**, *2*, 599–606.

[22] Liu, H.; Feng, Y.; Tanaka, T.; Urabe, Y.; Kataura, H. Diameter-selective metal/semiconductor separation of single-wall carbon nanotubes by agarose gel. *J. Phys. Chem. C* **2010**, *114*, 9270–9276.

[23] Miyata, Y.; Shiozawa, K.; Asada, Y.; Ohno, Y.; Kitaura, R.; Mizutani, T.; Shinohara, H. Length-sorted semiconducting carbon nanotubes for high-mobility thin film transistors. *Nano Res.* **2011**, *4*, 963–970.

[24] Krupke, R.; Hennrich, F.; Löhneysen, H. v.; Kappes, M. M. Separation of metallic from semiconducting single-walled carbon nanotubes. *Science* **2003**, *301*, 344–347.

[25] Arnold, M. S.; Green, A. A.; Hulvat, J. F.; Stupp, S. I.; Hersam, M. C. Sorting carbon nanotubes by electronic structure using density differentiation. *Nat. Nanotechnol.* **2006**, *1*, 60–65.

[26] Engel, M.; Small, J. P.; Steiner, M.; Freitag, M.; Green, A. A.; Hersam, M. C.; Avouris, P. Thin film nanotube transistors based on self-assembled, aligned, semiconducting carbon nanotube arrays. *ACS Nano* **2008**, *2*, 2445–2452.

[27] LeMieux, M. C.; Roberts, M.; Barman, S.; Jin, Y. W.; Kim, J. M.; Bao, Z. Self-sorted, aligned nanotube networks for thin-film transistors. *Science* **2008**, *321*, 101–104.

[28] Ju, S.; Doll, J.; Sharma, I.; Papadimitrakopoulos, F. Selection of carbon nanotubes with specific chiralities using helical assemblies of flavin mononucleotide. *Nat. Nanotechnol.* **2008**, *3*, 356–362.

[29] Lee, H. W.; Yoon, Y.; Park, S.; Oh, J. H.; Hong, S.; Liyanage, L. S.; Wang, H.; Morishita, S.; Patil, N.; Park, Y. J.; et al. Selective dispersion of high purity semiconducting single-walled carbon nanotubes with regioregular poly(3-alkylthiophene)s. *Nat. Commun.* **2011**, *2*, 541.

[30] Snow, E. S.; Novak, J. P.; Campbell, P. M.; Park, D. Random networks of carbon nanotubes as an electronic material. *Appl. Phys. Lett.* **2003**, *82*, 2145–2147.

[31] Izard, N.; Kazaoui, S.; Hata, K.; Okazaki, T.; Saito, T.; Iijima, S.; Minami, N. Semiconductor-enriched single wall carbon nanotube networks applied to field effect transistors. *Appl. Phys. Lett.* **2008**, *92*, 243112.

[32] Wang, C.; Zhang, J.; Ryu, K.; Badmaev, A.; De Arco, L. G.; Zhou, C. Wafer-scale fabrication of separated carbon nanotube thin-film transistors for display applications. *Nano Lett.* **2009**, *9*, 4285–4291.

[33] Kim, W.; Javey, A.; Tu, R.; Cao, J.; Wang, Q.; Dai, H. Electrical contacts to carbon nanotubes down to 1 nm in diameter. *Appl. Phys. Lett.* **2005**, *87*, 173101–173103.

[34] Richter, E.; Subbaswamy, K. R. Theory of size-dependent resonance Raman scattering from carbon nanotubes. *Phys. Rev. Lett.* **1997**, *79*, 2738–2741.

[35] Kataura, H.; Kumazawa, Y.; Maniwa, Y.; Umezu, I.; Suzuki, S.; Ohtsuka, Y.; Achiba, Y. Optical properties of single-wall carbon nanotubes. *Synth. Met.* **1999**, *103*, 2555–2558.

[36] Jorio, A.; Saito, R.; Hafner, J. H.; Lieber, C. M.; Hunter, M.; McClure, T.; Dresselhaus, G.; Dresselhaus, M. S. Structural ($n$, $m$) determination of isolated single-wall carbon nanotubes by resonant raman scattering. *Phys. Rev. Lett.* **2001**, *86*, 1118–1121.

[37] Wang, X.; Ouyang, Y.; Li, X.; Wang, H.; Guo, J.; Dai, H. Room-temperature all-semiconducting sub-10-nm graphene nanoribbon field-effect transistors. *Phys. Rev. Lett.* **2008**, *100*, 206803.